PERGAMON

International Journal of Solids and Structures 36 (1999) 2127–2141

INTERNATIONAL JOURNAL OF SOLIDS and STRUCTURES

Bending and buckling of superconducting partial toroidal field coils

J. S. Lee[a], X. J. Zheng[b,*]

[a] *Department of Civil and Environmental Engineering, Clarkson University, Potsdam NY 13699, U.S.A.*

[b] *Department of Mechanics, Lanzhou University, Lanzhou, 730000, P.R. China*

Received 4 April 1997; in revised form 22 September 1997

Abstract

Based on the theory of curved beams and the Biot–Savart law, a new theoretical model for magnetoelastic bending and buckling of superconducting toroidal field coils is developed and corroborated numerically. In contrast to the existing models, this model incorporates in-plane deformation of the coil. A semi-analytical approach is used to obtain the solution to the coupled problem. In order to validate the model and associated solution method, the experiment of Miya et al. (1982) is modeled. The theoretical predictions of the critical current of coils with none or one pin support are shown to be in excellent agreement with the published experimental data. It is also shown that the in-plane deformation has a significant influence on the critical current.

1. Introduction

Superconducting coils are used in many high energy devices such as thermonuclear magnetic fusion reactors, magnetic energy storage devices (SMES), magnetically levitated vehicles (Maglev), and superconducting generators (Moon, 1984). The dramatic rise of the magnetic field intensity achieved by superconducting magnets over conventional electromagnets has increased the ratio of magnetic forces to the load-carrying capacity and thus, raised concerns on the structural integrity. Minimization of the structural supports due to the stringent cooling requirement of superconducting magnets may further compromise the structural integrity. Thus, structural stability of superconducting magnets and associated supporting structures has become one of the most important design considerations for these devices.

In a Tokamak fusion reactor, a set of discrete superconducting coils is used to generate a toroidal

* Corresponding author.

0020–7683/99/$ - see front matter
PII: S0020–7683(97)00278–3

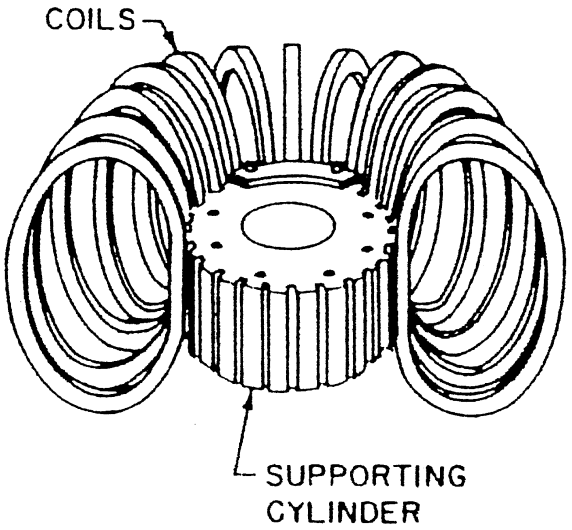

Fig. 1. Schematic drawing of toroidal field coils for fusion reactor.

magnetic field for plasma confinement (Fig. 1). Magnetic forces are generated due to the mutual interaction between the adjacent superconducting magnets. Experimental studies suggest that when the intensity of the superconducting current is small, the coil bends in its own plane. As the current becomes larger, a transverse bending deformation may occur. When the current reaches a critical value, the coil becomes structurally unstable. This phenomenon is referred to as the magnetoelastic instability and the critical value of the current may limit the design and safe operation of the fusion reactor. It is noted that this kind of out-of-plane bending may also occur when these exists a small misalignment of coils in the magnet system.

Experimental evidence of magnetoelastic instability of toroidal field coils was first demonstrated by Moon (1976). Moon also developed an analytical model for the magnetoelastic instability based on a dynamic method (Moon, 1976; Moon and Swanson, 1977), in which the critical current is determined when the natural frequency of lateral vibration of a coil becomes zero. Recently, Geiger and Jungst (1991) used the same method to investigate the TESPE toroidal magnets system, a torus with six D-shape superconducting coils of technologically relevant size and construction. A major limitation of this method is that it depends on the values of the natural frequency of the coil which are not easy to determine in practice for a large superconducting coil set in a full scale torus. Miya et al. (1980, 1982) developed a finite element model to study the magnetoelastic instability of superconducting toroidal field coils. They also conducted an experimental study with a three-coil partial torus and the magnetoelastic buckling current was predicted based on the parameters of the experimental device. However, their prediction of the critical current was not in good agreement with their experimental results. It should be noted that neither of the aforementioned analytical models included the in-plane extension and bending deformation. To date, it is still unclear how the in-plane deformation of the coil affects the critical current for magnetoelastic instability. We shall attempt in this paper to address this important question.

In what follows, we present a theoretical model for magnetoelastic interaction of super-

conducting toroidal field coils based on the theory of curved beams and Biot–Savart law. All possible modes of deformation (axial extension, in-plane bending, out-of-plane bending and torsion) of the coil are included in the model. A semi-analytical solution method is developed and described in detail. According to the nonlinear characteristic of magnetoelasticity, the critical current of magnetoelastic instability is predicted by the Southwell plot of the maximum transverse displacement in the out-of-plane of the coil. In order to ascertain the validation of the model, the experiment by Miya and his coworkers (1982) is modeled and numerical results are shown to be in excellent agreement with the experimental results.

2. Mechanics of coil

Consider a three-coil superconducting partial torus which consists of three D-shaped coils (shown in Fig. 2). The straight part of each coil is clamped, whereas the circular arc part is free, pin supported or clamped at some discrete locations. The current carrying coil m is placed symmetrically between two fixed current carrying coils l and r (here "m", "l" and "r" represent the middle, left hand side and right hand side, respectively). The coils are made by winding superconducting tapes of NbTi or Nb_3Sn thin multifilaments potted in copper matrix.

Before proceeding with the formulation for magnetic buckling of superconducting coils, we first make the following assumptions: (1) the coil is isotropic and homogeneous with equivalent elastic moduli; (2) the magnetic field arising from the current is constant; (3) the thickness of the coil is constant; (4) the current is uniformly distributed across the cross-section of the coil; (5) the distribution of the magnetic field in the coil can be treated as that of a normal conductor; (6) the cross-sectional dimension of the coil is much smaller than the distance between two adjacent coils. Although superconducting currents flow only on or near the surface of superconducting filaments, assumptions (4) and (5) may be reasonable since the coil is made of multifilaments which are more or less evenly distributed.

It is convenient to establish the basic equations of the problem in a local curved coordinate system $o\xi\eta\zeta$, in which ξ is along the circumferential axis of the coil and normal to the cross-section of the coil whereas η and ζ lie on the plane of the cross-section of the coil as shown in Fig. 2. Denoting the internal force vector $\mathbf{P}(\xi) = [N_\xi(\xi), Q_\eta(\xi), Q_\zeta(\xi), M_\xi(\xi), M_\eta(\xi), M_\xi(\xi)]^T$ and magnetic force vector $\mathbf{F}(\xi) = [-q_\xi, -q_\eta, -q_\zeta, -c_\xi, -c_\eta, -c_\zeta]^T$, the equilibrium equations for the center coil can be represented in matrix form:

$$\frac{\mathrm{d}\mathbf{P}(\xi)}{\mathrm{d}\xi} = \mathbf{A}\mathbf{P}(\xi) + \mathbf{F}(\xi) \tag{1}$$

in which

$$\mathbf{A} = \begin{bmatrix} 0 & 0 & -1/R & 0 & 0 & 0 \\ 0 & 0 & 0 & 0 & 0 & 0 \\ 1/R & 0 & 0 & 0 & 0 & 0 \\ 0 & 0 & 0 & 0 & 0 & -1/R \\ 0 & 0 & 1 & 0 & 0 & 0 \\ 0 & -1 & 0 & 1/R & 0 & 0 \end{bmatrix} \tag{2}$$

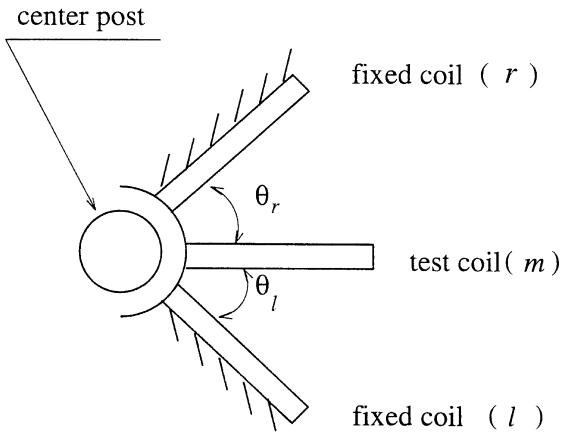

(a) Top View

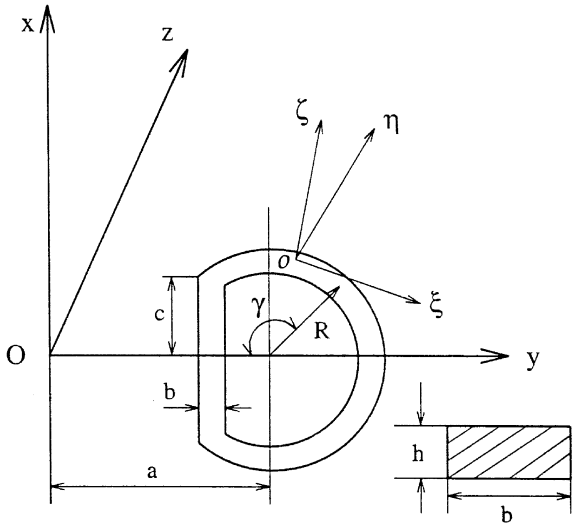

(b) Side View and Coordinate Systems

Fig. 2. Three-coil superconducting partial torus.

Taking the coupling effect among the axial extension, bending and torsion of the coil into account, we write the geometrical equations with constitutive relation in the following form:

$$\frac{\mathrm{d}u(\xi)}{\mathrm{d}\xi}+\frac{w(\xi)}{R}=\frac{N_{\xi}}{EF} \tag{3}$$

$$\frac{\mathrm{d}^2v(\xi)}{\mathrm{d}\xi^2}-\frac{\phi(\xi)}{R}=\frac{M_{\zeta}}{EJ_{\zeta}} \tag{4}$$

$$\frac{d^2w(\xi)}{d\xi^2} - \frac{2}{R}\frac{du(\xi)}{d\xi} - \frac{w(\xi)}{R} = -\frac{M_\eta}{EJ_\eta} \tag{5}$$

$$\frac{d\phi(\xi)}{d\xi} + \frac{1}{R}\frac{dv(\xi)}{d\xi} = \frac{M_\xi}{K} \tag{6}$$

in which, $u(\xi)$, $v(\xi)$ and $w(\xi)$ are components of displacement vector $\mathbf{U}(\xi)$ in the ξ-, η- and ζ-direction, respectively; F is the cross-section of the coil; J_η and J_ζ are the inertial moments of the section about the η- and ζ-axis, respectively; E is the equivalent axial Young's modulus of the superconducting coil; G is the equivalent shear elastic constant. The equivalent elastic constant E and G can be determined by the theory of composite materials from the elastic constants of the constituents, namely, superconducting of the superconducting composite filaments and copper matrix (Miya et al., 1980, 1982). In the above equation, $K = G\kappa$ is the torsional rigidity of the section about the ξ-axis where κ can be determined as the following:

$$\kappa = \frac{b^3h}{3} - \frac{64b^4}{\pi^5}\sum_{m=1,3,4,\ldots}^{\infty}\frac{1}{m^5}\tanh\frac{m\pi h}{2b} \tag{7}$$

where b and h are the width and height of the cross-section of the coil, respectively.

We recall that the coil is assumed to be clamped along the straight part as in the physical experiments (Miya et al., 1980). Denoting the two intersections between the straight part and the circular part by $\xi = \xi_\alpha$ and $\xi = \xi_\beta$, boundary conditions for the circular part of the coil can be written as

$$\xi = \xi_\alpha \quad \text{and} \quad \xi = \xi_\beta\text{:} \quad u(\xi) = 0, \quad v(\xi) = 0, \quad w(\xi) = 0 \tag{8}$$

$$\phi(\xi) = 0, \quad \frac{dv(\xi)}{d\xi} = 0, \quad \frac{dw(\xi)}{d\xi} = 0 \tag{9}$$

Equations (1) and (3)–(6) with 12 boundary conditions, (8) and (9), constitute the boundary-value problem for the coil system with no supports in the arc.

In the case when there is a support at the center of the arc (i.e. $\gamma = 180^\circ$), it suffices to consider only a half of the arc due to the symmetry. For a clamped support, we need to treat the coil section which is clamped at both ends ($\xi = \alpha$ and $\xi = 180^\circ$) and the boundary conditions are given by (8) and (9). For a pin supported at $\xi = 180^\circ$. The boundary conditions at the simply supported and are given by

$$\xi = 180^\circ\text{:} \quad \mathbf{U}(\xi) = 0, \quad \phi(\xi) = 0, \quad \frac{dw(\xi)}{d\xi} = 0, \quad M_\zeta(\xi) = 0 \tag{10}$$

3. Magnetic forces

We shall determine the magnetic body forces and moments on the centerline of the coil m due to calculating the magnetic field arising from the two outer coils with the aid of the Biot–Savart law. Consider two arbitrary points on the cross-sections F_l and F_m of the coils l and m, respectively.

Their position vectors relative to the center o_l and o_m of the sections are denoted by ρ_l and ρ_m, respectively. From the Biot–Savart law, the magnetic field on coil m by coil l can be written as

$$\mathbf{B}_l(\mathbf{r}_m) = \frac{\mu I_l}{4\pi}\int_{s_l}\frac{\mathrm{d}\mathbf{r}_l \times (\mathbf{r}_l^m + \rho_m - \rho_l)}{|\mathbf{r}_l^m + \rho_m - \rho_l|^3} \tag{11}$$

and the Lorentz force and moment, respectively, become

$$\begin{aligned}\mathbf{q}_l(\mathbf{r}_m) &= I\mathbf{e}_\xi \times \mathbf{B}_l(\mathbf{r}_m)\\ &= \frac{\mu I_l I_m}{4\pi F_l F_m}\int_{F_l}\int_{s_l}\int_{F_m}\mathbf{e}_\xi \times \left[\frac{\mathrm{d}\mathbf{r}_l \times (\mathbf{r}_l^m + \rho_m - \rho_l)}{|\mathbf{r}_l^m + \rho_m - \rho_l|^3}\right]\mathrm{d}F_l\,\mathrm{d}F_m\end{aligned} \tag{12}$$

and

$$\mathbf{c}_l(\mathbf{r}_m) = \frac{\mu I_l I_m}{4\pi F_l F_m}\int_{F_l}\int_{s_l}\int_{F_m}\rho_m \times \left[\mathbf{e}_\xi \times \frac{\mathrm{d}\mathbf{r}_l \times (\mathbf{r}_l^m + \rho_m - \rho_l)}{|\mathbf{r}_l^m + \rho_m - \rho_l|^3}\right]\mathrm{d}F_l\,\mathrm{d}F_m \tag{13}$$

where $\mathbf{r}_l$ is the position vector of coil l and $\mathbf{r}_l^m$ is the relative position vector of the centerlines of coils l and m. Since

$$\int_{F_l}\rho_l\,\mathrm{d}F_l = 0, \quad \int_{F_m}\rho_m\,\mathrm{d}F_m = 0 \tag{14}$$

and $\mathbf{e}_\xi$ is normal to ρ_m, we can show that $\mathbf{c}_l(\mathbf{r}_m) \equiv 0$. Since $|\rho_l| \ll |\mathbf{r}_l^m|$ and $|\rho_m| \ll |\mathbf{r}_l^m|$ from the assumption (6) mentioned above, (12) can be expressed as

$$\mathbf{q}_l(\mathbf{r}_m) = \frac{\mu I_l I_m}{4\pi}\int_{s_l}\mathbf{e}_\xi \times \left[\frac{\mathrm{d}\mathbf{r}_l \times \mathbf{r}_l^m}{(\mathbf{r}_l^m)^3}\right] \tag{15}$$

Taking the same consideration for coil r, we obtain the total Lorentz force acting on coil m by coils l and r as

$$\mathbf{q}(\mathbf{r}_m) = \frac{\mu I_l I_m}{4\pi}\int_{s_l}\mathbf{e}_\xi \times \left[\frac{\mathrm{d}\mathbf{r}_l \times \mathbf{r}_l^m}{(\mathbf{r}_l^m)^3}\right] + \frac{\mu I_r I_m}{4\pi}\int_{s_r}\mathbf{e}_\xi \times \left[\frac{\mathrm{d}\mathbf{r}_r \times \mathbf{r}_r^m}{(\mathbf{r}_r^m)^3}\right] \tag{16}$$

It should be noted that, when calculating the magnetic force by (16), $\mathbf{r}_l$, $\mathbf{r}_r$, $\mathbf{r}_l^m$ and $\mathbf{r}_r^m$ should be written in the local coordinate system. Moreover, we must also take into account the effect of deformation of coil m on the magnetic force. This can be accomplished by writing the relative position vector as follows:

$$\mathbf{r}_l^m = \mathbf{r}_m + \mathbf{U}(\xi) - \mathbf{r}_l, \quad \mathbf{r}_r^m = \mathbf{r}_m + \mathbf{U}(\xi) - \mathbf{r}_r \tag{17}$$

Note that the magnetical force and the deformation of coil m are thus, mutually coupled; that is, the magnetic force effects the deformation of coil m and, conversely, the deformation of the coil influences the magnetic force. Consequently, the basic equations of the problem are inherently nonlinear, even when each subsystem (mechanical and electromagnetic) is considered to be linear.

Since the D-shape coil in torus are of the same geometrical size and placed symmetrically, and carrying the same current (i.e., $I_l = I_m = I_r = I, \theta_l = \theta_r$), there exists a trivial solution to eqns (1) and (3)–(6) for out-of-plane bending. Consider an arbitrary pair of symmetry points on coil l and r. When $\theta_l = \theta_r$ and $v(\xi) \equiv 0$, we have

$$(r_l^m)_\xi = (r_r^m)_\xi, \quad (r_l^m)_\eta = -(r_r^m)_\eta, \quad (r_l^m)_\zeta = (r_r^m)_\zeta \tag{18}$$

$$\mathrm{d}(r_l)_\xi = \mathrm{d}(r_r)_\xi, \quad \mathrm{d}(r_l)_\eta = -\mathrm{d}(r_r)_\eta, \quad \mathrm{d}(r_l)_\zeta = \mathrm{d}(r_r)_\zeta \tag{19}$$

and $r_l^m = r_r^m$. Therefore, the expression (16) can be rewritten as

$$\begin{aligned}\mathbf{q}(\mathbf{r}_m) &= \frac{\mu I^2}{4\pi}\int_{s_l} \mathbf{e}_\xi \times \left[\frac{\mathrm{d}\mathbf{r}_l \times \mathbf{r}_l^m}{(r_l^m)^3} + \frac{\mathrm{d}\mathbf{r}_r \times \mathbf{r}_r^m}{(r_r^m)^3}\right] \\ &= \frac{\mu I^2}{4\pi}\int_{s_l} \frac{2}{(r_l^m)^3}[(r_l^m)_\zeta \,\mathrm{d}(r_l)_\xi - (r_l^m)_\xi \,\mathrm{d}(r_l)_\zeta]\mathbf{e}_\zeta\end{aligned} \tag{20}$$

which shows that there is no transverse magnetic force acting on coil m when the outer coils are symmetrically placed and $v(\xi) \equiv 0$. Thus, a trivial solution always exists for out-of-plane deflection. However, since the governing equations are nonlinear, it is possible that a nontrivial solution for transverse bending deformation may exist when the applied current approaches a critical value. We shall pay special attention to this non-trivial solution to examine the buckling phenomenon.

4. Solution method

A semi-analytical and semi-numerical method is used here to obtain a solution of the coil for a given magnetic force. We first obtain exact homogeneous solutions to the basic equations in closed form. The finite difference method is then used to obtain the solution to the nonhomogeneous problem. Finally, the integral constants are determined by the initial parameter method. Once the solutions, which are based on a set of assumed initial displacement of the coil, to eqn (1) and (3)–(6) for a given current are obtained, an iterative method can then be used to find the true solution for a given current since the problem is coupled.

4.1. Homogeneous solution

The exact homogeneous solution to (1), denoted by $\mathbf{P}^* = [N_\xi^*(\xi), \quad Q_\eta^*(\xi), \quad Q_\zeta^*(\xi), \; M_\xi^*(\xi), \; M_\eta^*(\xi), \; M_\zeta^*(\xi)]^T$, can be expressed in the following form:

$$\mathbf{P}^*(\xi) = \mathbf{T}_{11}(\xi)\mathbf{C}_1 \tag{21}$$

in which $\mathbf{C}_1 = [C_1, C_2, C_3, C_4, C_5, C_6]^T$ is an unknown constant vector, and

$$\mathbf{T}_{11} = \begin{bmatrix} 0 & \sin\frac{\xi}{R} & \cos\frac{\xi}{R} & 0 & 0 & 0 \\ 1 & 0 & 0 & 0 & 0 & 0 \\ 0 & -\cos\frac{\xi}{R} & \sin\frac{\xi}{R} & 0 & 0 & 0 \\ 0 & 0 & 0 & 0 & \sin\frac{\xi}{R} & \cos\frac{\xi}{R} \\ 0 & -R\sin\frac{\xi}{R} & -R\cos\frac{\xi}{R} & 1 & 0 & 0 \\ 0 & 0 & 0 & 0 & -\cos\frac{\xi}{R} & \sin\frac{\xi}{R} \end{bmatrix} \tag{22}$$

The exact homogeneous solution to (3)–(6), noted by $\Psi^*(\xi) = [u^*, \phi^*, v^*, \mathrm{d}v^*/\mathrm{d}\xi, w^*, \mathrm{d}w^*/\mathrm{d}\xi]^T$, can be written in the following form:

$$\Psi^*(\xi) = [T_{21}(\xi), T_{22}(\xi)] \begin{bmatrix} \mathbf{C}_1 \\ \mathbf{C}_2 \end{bmatrix} \tag{23}$$

where $\mathbf{C}_2 = [C_7, C_8, C_9, C_{10}, C_{11}, C_{12}]^T$ is an unknown constant vector, and

$$\mathbf{T}_{21}(\xi) = \begin{bmatrix} 0 & t_{1s} + t_1\cos\frac{\xi}{R} & t_{1c} - t_1\sin\frac{\xi}{R} & \frac{R\xi}{EJ_\eta} & 0 & 0 \\ 0 & 0 & 0 & 0 & t_{2s} - t_2\cos\frac{\xi}{R} & t_{2c} + t_2\sin\frac{\xi}{R} \\ \frac{R^2\xi}{K} & 0 & 0 & 0 & -Rt_{2s} - \frac{R^2}{\xi}t_{2c} & \frac{R^2 t_{2s}}{\xi} - Rt_{2c} \\ \frac{R^2}{K} & 0 & 0 & 0 & -Rt_{2c} & Rt_{2s} \\ 0 & -t_{1c} & t_{1s} & \frac{R^2}{EJ_\eta} & 0 & 0 \\ 0 & \frac{-t_{1c}}{\xi} + \frac{t_{1s}}{R} & \frac{t_{1s}}{R} + \frac{t_{1c}}{\xi} & 0 & 0 & 0 \end{bmatrix} \tag{24}$$

$$\mathbf{T}_{22}(\xi)=\begin{bmatrix} 1 & \cos\frac{\xi}{R} & -\sin\frac{\xi}{R} & 0 & 0 & 0 \\ 0 & 0 & 0 & 0 & \cos\frac{\xi}{R} & -\sin\frac{\xi}{R} \\ 0 & 0 & 0 & 0 & -R\cos\frac{\xi}{R} & R\sin\frac{\xi}{R} \\ 0 & 0 & 0 & 1 & \sin\frac{\xi}{R} & \cos\frac{\xi}{R} \\ 0 & \sin\frac{\xi}{R} & \cos\frac{\xi}{R} & 0 & 0 & 0 \\ 0 & \frac{1}{R}\cos\frac{\xi}{R} & -\frac{1}{R}\sin\frac{\xi}{R} & 0 & 0 & 0 \end{bmatrix} \tag{25}$$

in which

$$D_1=\frac{2}{EFR}+\frac{R}{EJ_\eta};\quad D_2=\frac{1}{ERJ_\zeta}+\frac{1}{KR} \tag{26}$$

$$t_1=\frac{D_1R^2}{2}-\frac{R}{EF},\quad t_2=\frac{D_2R^2}{2}-\frac{R}{EJ_\zeta} \tag{27}$$

$$t_{1s}=\frac{D_1R\xi}{2}\sin\frac{\xi}{R},\quad t_{1c}=\frac{D_1R\xi}{2}\cos\frac{\xi}{R} \tag{28}$$

$$t_{2s}=\frac{D_2R\xi}{2}\sin\frac{\xi}{R},\quad t_{2c}=\frac{D_2R\xi}{2}\cos\frac{\xi}{R} \tag{29}$$

Solution (22) and (24) can be combined and written in the following form:

$$\mathbf{\Phi}^*(\xi)=\mathbf{TC} \tag{30}$$

where

$$\mathbf{\Phi}^*(\xi)=\begin{Bmatrix}\mathbf{P}^*(\xi)\\ \mathbf{\Psi}^*(\xi)\end{Bmatrix}\quad \mathbf{T}(\xi)=\begin{bmatrix}\mathbf{T}_{11}(\xi) & \mathbf{T}_{12}(\xi)\\ \mathbf{T}_{21}(\xi) & \mathbf{T}_{22}(\xi)\end{bmatrix}\quad \mathbf{C}=\begin{Bmatrix}\mathbf{C}_1\\ \mathbf{C}_2\end{Bmatrix} \tag{31}$$

In the above, $\mathbf{T}_{12}(\xi)$ is a 6×6 null matrix. Equation (3) represents the exact solution to the homogeneous problem (1) and (3)–(6) in closed form.

4.2. Inhomogeneous solutions

The finite difference method is used to obtain the inhomogeneous solution to eqns (1) and (3)–(6) for an arbitrary applied load $\mathbf{F}(\xi)$. The inhomogeneous solution is then added to the homogeneous solution given by (30), and the integral constants are determined by applying the boundary and support conditions.

Let us divide the coil m into s element such that

$$\xi_\alpha < \xi_1 < \xi_2 < \cdots < \xi_{s-1} < \xi_s = \xi_\beta \tag{32}$$

The differential eqns (1) and (3)–(6) can be transfered into algebraic ones for each element. We can get the values of $\mathbf{P}(\xi)$ and $\mathbf{\Psi}(\xi)$ on each node by resolving these algebraic equations. These inhomogeneous solutions can be written in the following form:

$$\bar{\mathbf{\Phi}}(\xi_j) = \begin{Bmatrix} \bar{\mathbf{P}}(\xi_j) \\ \bar{\mathbf{\Psi}}(\xi_j) \end{Bmatrix}, \quad j = 1, 2, \ldots, s \tag{33}$$

The complete solution to eqn (1) and eqns (3)–(6) can then be written as

$$\mathbf{\Phi}(\xi) = \mathbf{\Phi}^*(\xi) + \bar{\mathbf{\Phi}}(\xi) = \mathbf{T}(\xi)\mathbf{C} + \bar{\mathbf{\Phi}}(\xi) \tag{34}$$

4.3. The initial parameter method

Here, we shall adopt the initial parameter method (Vlasov and Leontev, 1966) to determine the vector $\mathbf{C}$ which consists of 12 unknown constants for the single arc circular coil. Substituting the boundary conditions at $\xi = \xi_\alpha$ into eqn (34), we can express $\mathbf{C}$ as

$$\mathbf{C} = [\mathbf{T}(\xi_\alpha)]^{-1}\mathbf{\Phi}(\xi_\alpha) - [\mathbf{T}(\xi_\alpha)]^{-1}\bar{\mathbf{\Phi}}(\xi_\alpha) \tag{35}$$

where $\mathbf{\Phi}(\xi_\alpha)$ is the initial parameter matrix. The solution (34) can then be expressed in terms of the initial parameter as follows:

$$\mathbf{C} = \mathbf{G}(\xi)\mathbf{\Phi}(\xi_\alpha) - \mathbf{G}(\xi)\bar{\mathbf{\Phi}}(\xi_\alpha) + \bar{\mathbf{\Phi}}(\xi) \tag{36}$$

in which

$$\mathbf{G}(\xi) = \mathbf{T}(\xi)\mathbf{T}^{-1}(\xi_\alpha) \tag{37}$$

It is noted that from the twelve elements of the initial parameter matrix $\mathbf{\Phi}(\xi_\alpha)$, six elements are given by the boundary conditions at $\xi = \xi_\alpha$ and the rest can be determined by the boundary conditions at $\xi = \xi_\beta$.

4.4. Iterative method

So far, the solution procedure is based on the assumption that the magnetic forces are known *a priori*. However, magnetic forces acting on coil m depends on the current configuration of the coil. Consequently, magnetic forces are not known until the deformation of the coil is determined. In order to treat this coupled problem, we employ an iterative technique: we first calculate the magnetic force $\mathbf{q} = \mathbf{q}_n$ by eqn (16) for a given displacement $\mathbf{U} = \mathbf{U}_n$; we then calculate a new displacement $\mathbf{U} = \mathbf{U}_{n+1}$ for the magnetic force $\mathbf{q}_n$ by using the procedure described above until the solution converges, i.e., the condition

$$|\mathbf{U}_{n+1} - \mathbf{U}_n| < \delta \tag{38}$$

is satisfied, where $0 < \delta \ll 1$ is a prescribed tolerance, and n denotes the number of iterations.

5. Numerical results

In order to confirm the validity of our theoretical model and the semi-analytical solution method, the experiment by Miya and his coworkers (1982) is modeled here. Material and geometrical parameters used in the calculation are as follows: $E = 2.7 \times 10^{10}$ Pa; $G = 3.4 \times 10^{9}$ Pa; $\theta_r = \theta_l = 22.5^{\circ}$; $h = 0.6$ mm; $a = 90$ mm; $b = 9$ mm; and $c = 40$ mm. We consider three different support conditions: no support; a pin support; and a clamp support in the circular arc section. Assuming that symmetrically placed supports would perform better than unsymmetrically placed ones, we consider only the former in this study. That is, in the case when there is a support in the arc section, the support is located on the y axis (i.e.$\gamma = 180^{\circ}$, as shown in Fig. 2).

Distribution of the three displacement and three internal force components in the coil can be obtained by the present model. For example, distribution of the three displacement components in the coil with a pin support is shown in Fig. 3. Due to the symmetry of the geometry and the magnetic field in the middle coil about the y–o–z plane, displacement and internal force distributions exhibit the same symmetry as expected. As shown in the figure, the transverse displacement of the coil is much larger than the in-plane ones. Therefore, we shall pay close attention to the transverse deformation which renders the coil system unsymmetric. It is reminded, however, that we cannot neglect the effect of the in-plane deformation as will be shown below.

Calculation of the transverse deflection is carried out until the superconducting current reaches a critical value. Note that there is a notable increase as the applied current approaches the critical one. The maximum transverse deflection is plotted as a function of the applied current for three cases in Fig. 4. From these curves, we confirm that the relationship between the deformation with

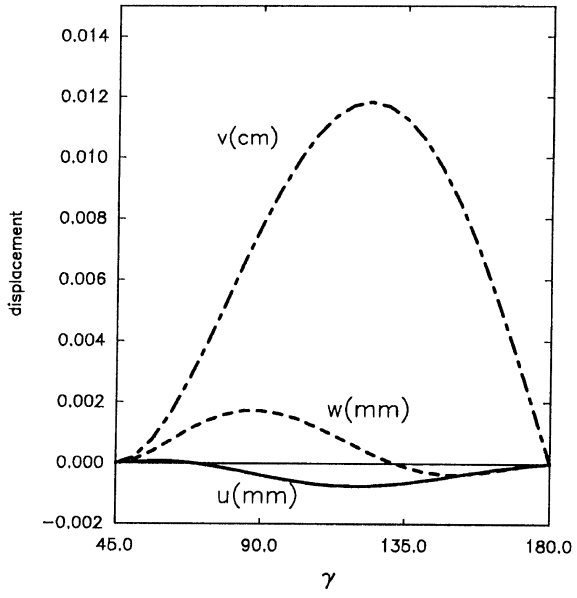

Fig. 3. Distribution of the three displacement components in the coil with one pin support (I = 100 A/turn).

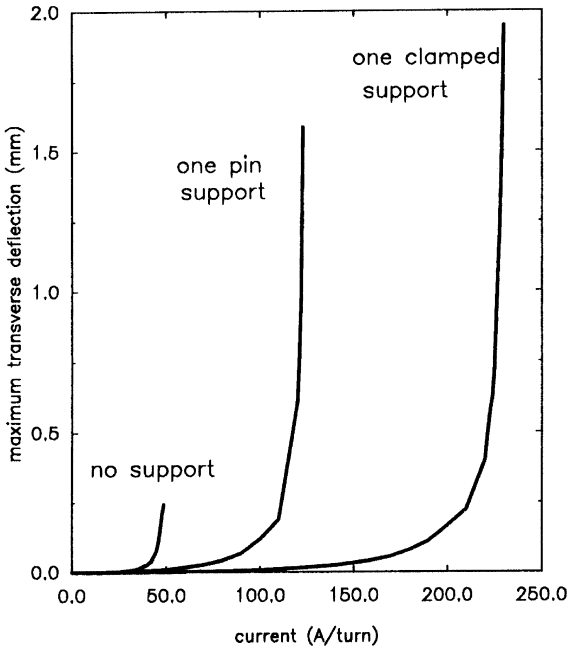

Fig. 4. The maximum transverse deflection vs the applied current.

the applied current is nonlinear. As shown in the figure, the coil first buckles, then bends nonlinearly varying with the square of the applied current, and finally snaps or losses stability. This characteristic of the nonlinear magnetoelastic interaction is similar to that of an axially compressed column with nonlinear geometrical deformation in which the buckling state is stable. Here, the buckling mode is the same as the deformation configuration as shown in Fig. 3 for one pin support. Although this deformation behavior was observed experimentally (Moon, 1976, 1979; Miya et al., 1982), no theoretical models have been able to simulate this behavior to date.

In order to determine the critical current, the Southwell plots are made for the three cases in Fig. 5. The slope of this plot could give the critical current. From Fig. 5, we find that the critical current of the coil without support is much lower than those of the coils with a support. It is shown that the critical current for the coil with a clamped support is much higher (almost twice as large) than that of the coil with a pin support.

Comparisons between our theoretical predictions and the existing results, both theoretical and experimental, for the critical values of magnetoelastic snapping current of the three-coil superconducting partial torus are summarized in Table 1. The values obtained from our analysis are slightly higher than experimental data with a relative error 3.14% for the coil with no support and 0.35% for the coil with a pin support. It is reasonable to argue that theoretical predictions of the critical current are higher than the corresponding experimental values because small lateral misalignments are inevitable in physical tests, which tend to lower the critical values (Zhou and Miya, 1997). The theoretical results of Miya et al. (1980, 1982) are also listed for comparison to ascertain the importance of the effect of the in-plane deformation on the critical current. Since the

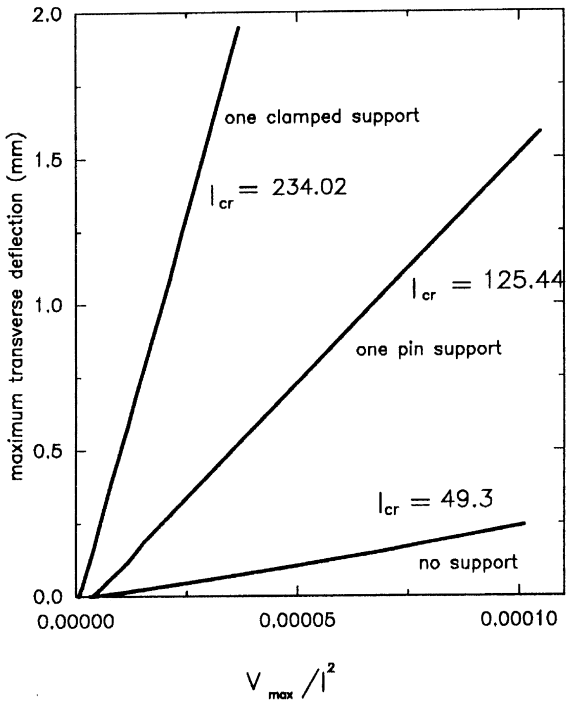

Fig. 5. Southwell plots for critical current.

Table 1
Comparison of critical current (I_{cr} A/turn)

Three coil torus	Experiment (Miya et al.)	Theoretical results (error in %)	
		Miya et al.	Present analysis
No support	47.8	37 (−22.6)	49.3 (3.14)
One pin support	125.0	108 (−13.6)	125.44 (0.35)
One clamped support	NA	NA	234.02 (NA)

in-plane deformation was neglected in their model, their predicted values are considerably lower than the experimental data with a relative error of 22.6% for the coil with no support and 13.6% for the coil with a pin support. Hence, we can state that the effect of in-plane deformation on the critical current is significant even though magnitude of the in-plane deformation is much smaller than that of the out-of-plane deformation.

6. Conclusions

Magnetoelastic behavior of a superconducting three-coil partial torus with different support conditions were considered in this paper. With the aid of the Biot–Savart law and the theory of curved beams, we presented a new theoretical model which can describe the in-plane and out-of-plane deformation of the coil as well as the internal forces in the coil. A semi-analytical solution method was developed combining an exact closed-form solution, the finite difference method, the initial parameter method and the iterative technique to solve the coupled nonlinear problem. The model is shown to be capable of predicting the deformation process of the coil as observed by existing experiments for the first time. The critical currents of the coil obtained in this paper are in better agreement with the existing experimental data than the hitherto reported here are better founded.

Acknowledgements

This research was supported in part by the National Science Foundation under Grant MSS-9313216 and grants from the Chinese National Nature Science Foundation for outstanding youth and the Science Foundation of the National Education Committee of China for outstanding teacher. The authors gratefully acknowledge the support.

References

Geiger, W., Jungst, K.P., 1991. Buckling calculations and measurements on a technologically relevant toroidal magnet system. ASME Journal of Applied Mechanics 58, 167–174.

Miya, K., Takagi, T., 1978. Finite element analysis of electromagnetoelastic buckling of a superconducting magnet in a magnetic fusion reactor. ASME PVP-PB-031 Computer Technology in Fusion Energy Research, pp. 1–24.

Miya, K., Uesaka, M., 1982. An application of a finite element method to magnetomechanics of superconducting magnets for magnetic reactors. Nuclear Engineering and Design 72, 275–296.

Miya, K., Takagi, T., Uesaka, M., 1980. Finite element analysis of magnetoelastic buckling and experiments on a three-coil superconducting partial torus. Mechanics of Superconducting Structures, F.C. Moon (Ed.), pp. 91–107. ASME, New York.

Miya, K., Uesaka, M., Moon, F.C., 1982. Finite element analysis of vibration of toroidal field coils coupled with Laplace transform. ASME Journal of Applied Mechanics 49, 594–600.

Moon, F.C,. 1976. Buckling of a superconducting coil nested in a three-coil toroidal segment. Journal of Applied Physics 47, 920–921.

Moon, F.C., 1979. Experiments on magnetoelastic buckling in a superconducting torus. ASME Journal of Applied Mechanics 46, 145–151.

Moon, F.C. 1979. Buckling of a superconducting ring in a toroidal magnetic field. ASME Journal of Applied Mechanics 46, 151–155.

Moon, F.C., 1980. Magnetoelastic instables in superconducting structures and Earnshaw's theorem. Mechanics of Superconducting Structures, F. C. Moon (Ed.), pp. 77–90.

Moon, F.C., 1984. Magneto-solid Mechanics. John Wiley and Sons, New York.

Moon, F.C., Swanson, C. 1977. Experiments on buckling and vibration of superconducting coils. ASME Journal of Applied Mechanics 44, 707–713.

Swanson, C., Moon, F.C., 1977. Buckling and vibration in a five coil superconducting partial torus. Journal of Applied Physics 48, 3110–3115.

Vlasov, V.Z., Leontev, N.N., 1966. Beams, Plates and Shells on Elastic Foundations. NASA TTF-357, TT65-50135.

Zhou, Y.H., Miya, K. 1997. Mechanical behavior of magnetoelastic interaction for superconducting helical magnets. Fusion Engineering and Design, in press.